Supporting information for:

Simple and rational design of polymer nano-platform for high performance of HCV related miR-122 reduction in liver

Hao Fu [†], *XiangYu Zhang*[†], *Qi Wang*[‡], *Yin Sun*[†], *Lei Liu*[†], *LiLi Huang*[†], *Li Ding*[†], *Ming Shen*[†], *Lin Zhang*[*,§], *Yourong Duan*[*,†]

[†]State Key Laboratory of Oncogenes and Related Genes, Renji Hospital, School of Biomedical Engineering, Shanghai Jiao Tong University

[‡]Key Laboratory for Advanced Materials and Institute of Fine Chemicals, Shanghai Key Laboratory of Functional Materials Chemistry, School of Chemistry and Molecular Engineering, East China University of Science and Technology

[§]Beijing Tsinghua Changgung Hospital, School of Clinical Medicine, Tsinghua University

***Corresponding authors:**

You-Rong Duan

State Key Laboratory of Oncogenes and Related Genes, Shanghai Cancer Institute, Renji Hospital, School of Medicine, Shanghai Jiao Tong University, Shanghai 200032 (P. R. China)

E-mail: yrduan@shsci.org

Lin Zhang,

Beijing Tsinghua Changgung Hospital, School of Clinical Medicine, Tsinghua University, No. 168 Litang Road, Changping District, Beijing 102218 (P. R. China)

E-mail: zla02285@btch.edu.cn

Supplementary Figures:

Table S1. AN-loaded mPEG-b-PLGA-b-PLL nanoparticle formulations and properties

Formulation	antimiR in feed (nmol)	EE (%)	DL (%)	Size(nm)	PDI	Zeta potential(mV)
$NP_{2.5}$	2.5	> 90	0.213	118.5	0.204	+22
$NP_{5.0}$	5	> 85	0.426	136.2	0.241	-5.4
$NP_{10.0}$	10	> 80	0.851	155.7	0.268	-12

Table S2. IN-loaded mPEG-b-PLGA-b-PLL nanoparticle formulations and properties

Formulation	antimiR in feed (nmol)	EE (%)	DL (%)	Size(nm)	PDI	Zeta potential(mV)
$NP_{2.5}$	2.5	> 90	0.204	120.9	0.192	+24
$NP_{5.0}$	5	> 80	0.417	140.6	0.217	-4.2
$NP_{10.0}$	10	> 80	0.824	153.1	0.253	-10.5

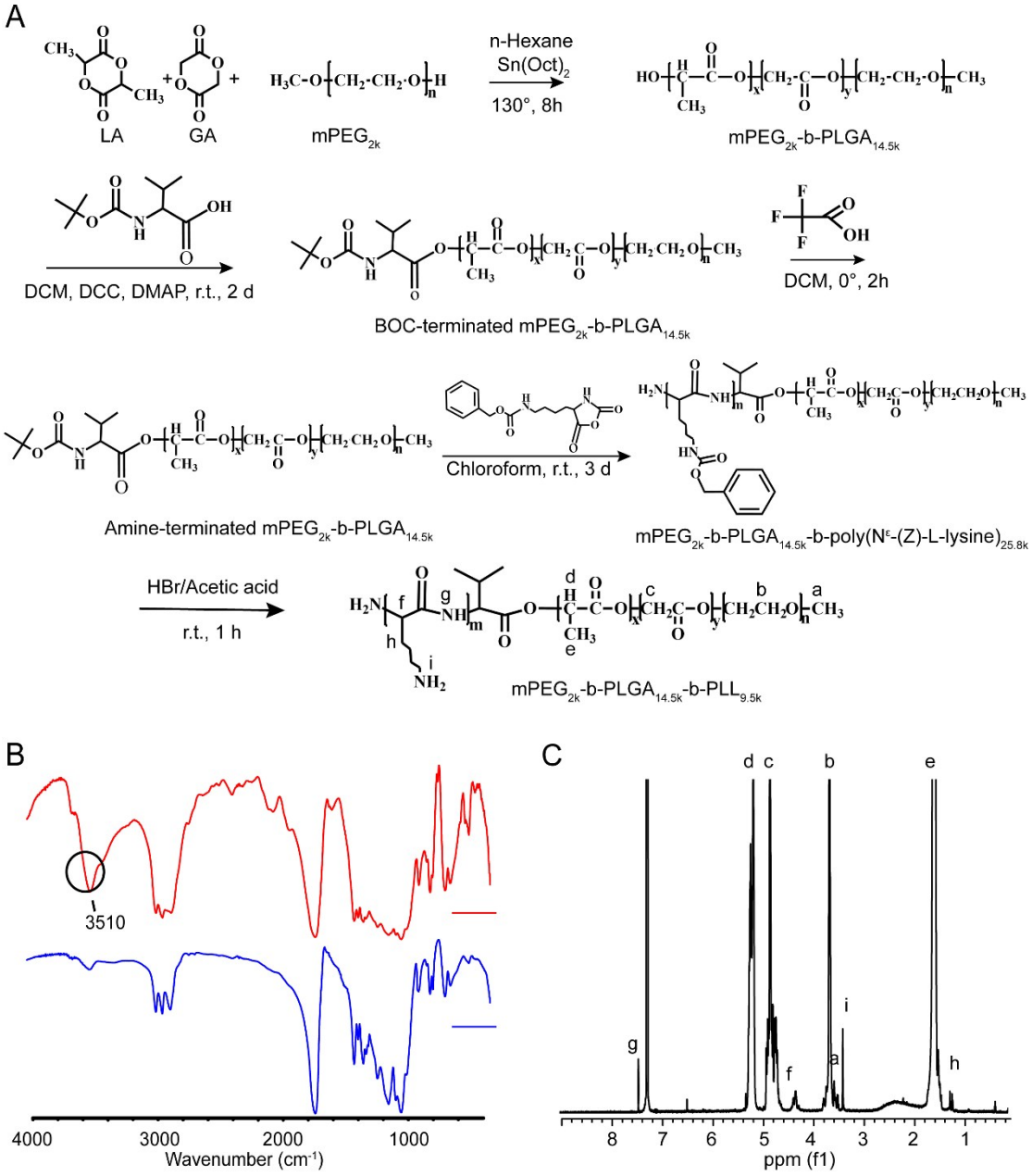

Fig. S1 Synthesis of mPEG-PLGA-b-PLL block copolymer and characteristics of mPEG-PLGA-b-PLL block copolymer (A). FTIR spectrum of mPEG-PLGA (Red), mPEG-PLGA-b-PLL (Blue) (B). The absorption peak at 3510 cm^{-1} was attributed to the -NH- stretch vibration, indicating the mPEG-PLGA-b-PLL was synthesized. 1H NMR spectrum of mPEG-PLGA-b-PLL block copolymer (C). The peaks at 4.36 ppm, (f, -CH-), 3.38 ppm (i, -CH2-) and 1.35 ppm (h, -CH2-) were attributed to protons of the lysine segment. The peaks at 7.87 (g, -NH-) ppm were assigned to protons of the amino group of the lysine group (C).

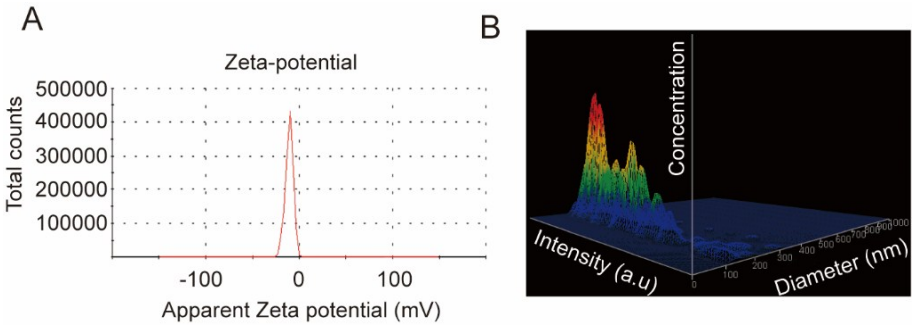

Fig. S2 Characteristics of NPs. (A) The Zeta-potential of NP-AN was -12 mV. (B) The size distribution results of Nanosight showed similar sizes in the distribution results.

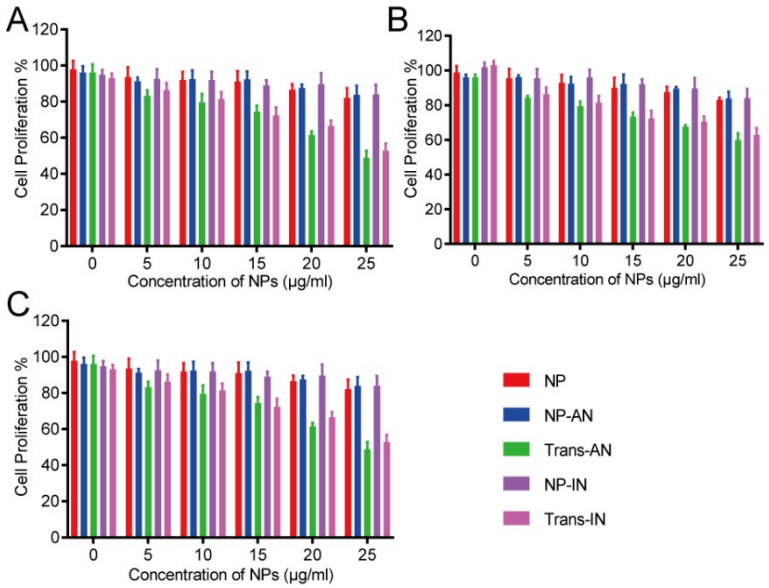

Fig. S3 (A), (B), (C) MTT results of NPs for 24, 48 and 72 h. The viability of cells incubated with anti-miRs-loaded NPs were all above 80%, which showed nearly no toxicity to LO2 cells. Data are presented as the means ± SD. (n=3). NP, NP-AN, Trans-AN, NP-IN and Trans-IN means injected with empty nanoparticles, antagomir-loaded nanoparticles, transfection agent with antagomir-122, inhibitor-loaded nanoparticles and transfection agent with inhibitor-122.

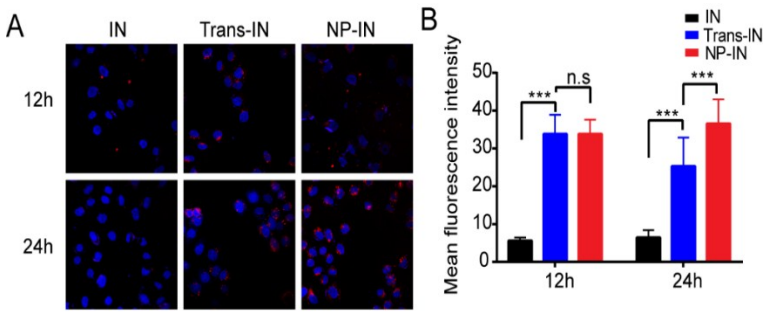

Fig. S4 Cellular uptake of NPs and lysosome escape of NPs. (A) LO2 cells treated with different IN, transfection agent with IN and NP-IN for 12 and 24h. (B) Quantitative results of cellular uptake of A, which further qualified the results from A.

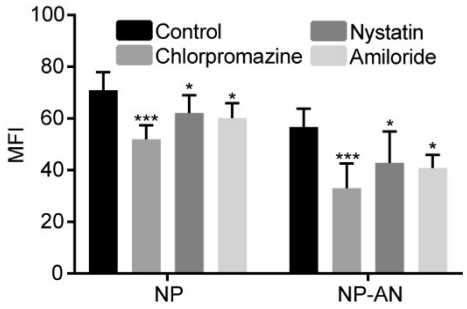

Fig. S5 Investigation of internalization pathways of NP and NP-AN.

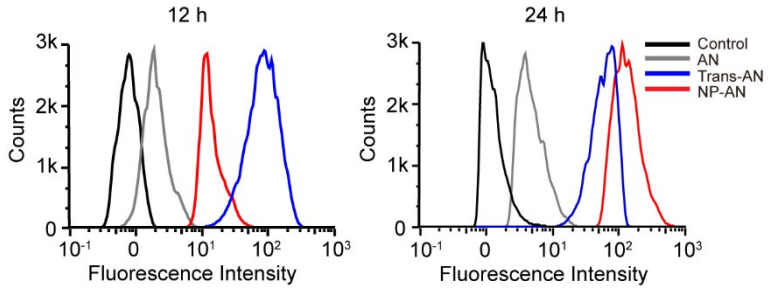

Fig. S6 Cellular uptake results measured by flowcytometry of NP-AN. The result was consist with the result at (A). (D) showed that NPs were trapped at lysosome at 4 h, as the red and green fluorescence were overlaid together.

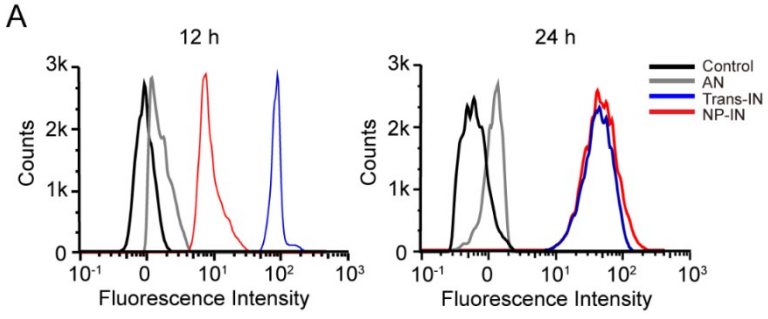

Fig. S7 Cellular uptake results measured by flowcytometry . (A) LO2 cells treated with IN with/without NPs and transfection agent for 12h. (B) LO2 cells treated with inhibitor with/without NPs and transfection agent for 24h.

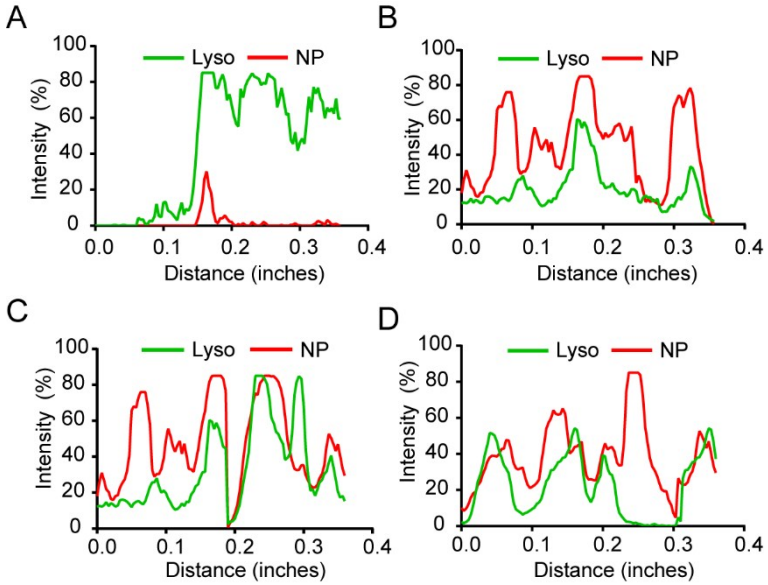

Fig. S8 Lysosome escape was performed at 8 and 12 h, while the green and red fluorescence began to depart after 1 h (A), 8 h (B), 12 h (C) and 24 h (D).

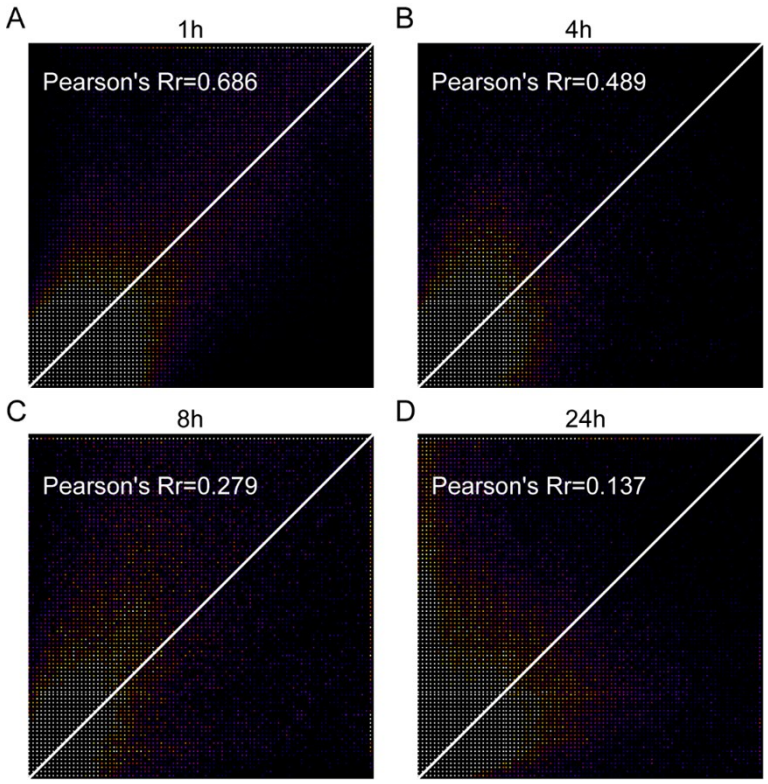

Fig. S9 Scatter plot of Figure 2D. (A) Scatter plot calculated from Figure 2D merged picture of 1h; (B) Scatter plot calculated from Figure 2D merged picture of 4h; (C) Scatter plot calculated from Figure 2D merged picture of 8h; (D) Scatter plot calculated from Figure 2D merged picture of 24h.

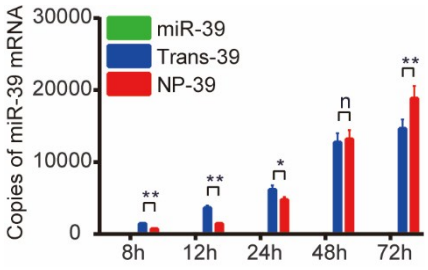

Fig. S10 Exogenous microRNA transfection in vitro. LO2 cells treated with miR-39 mimic (miR-39), transfection agent with miR-39 mimic (Trans-39) and miR-39 mimic loaded NPs (NP-39).

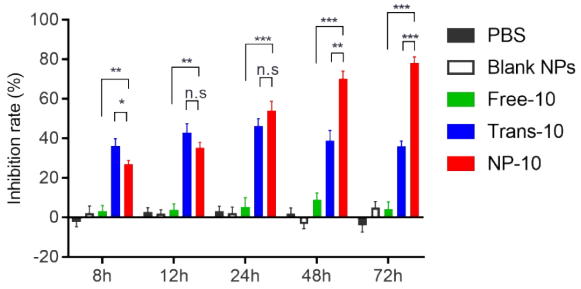

Fig. S11 LO2 cells treated with inhibitor (IN), transfection agent with IN and IN loaded NPs (NP-IN), miR-122 inhibition were measured.

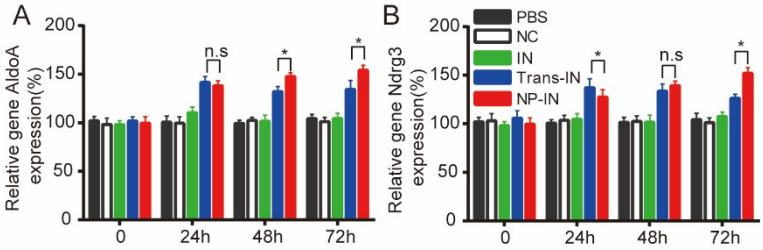

Fig. S12 LO2 cells treated with inhibitor (IN), transfection agent with IN and IN loaded NPs (NP-IN), Aldoa and Ndrg3 expression were measured. (A) Relative Aldoa expression after incubation. (B) Relative Ndrg3 expression after incubation.

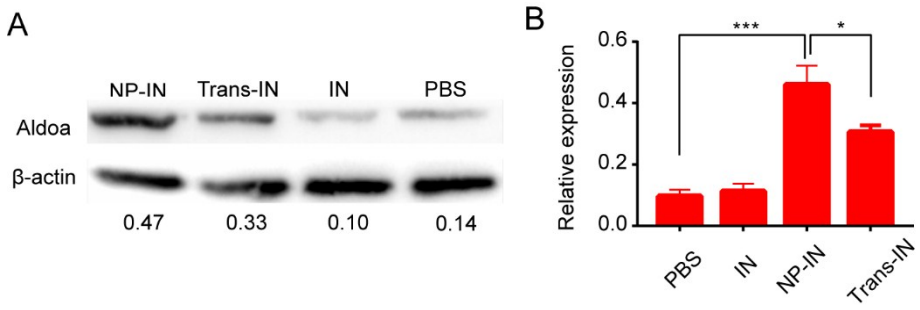

Fig. S13 (A) The Aldoa protein expression after different treatments. Aldoa protein level increased dramatically within 3 weeks after administrated with NP-IN. (B) Quantitative results of A

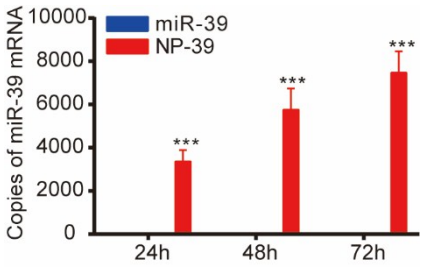

Fig. S14 Exogenous microRNA transfection *in vivo*. Balb/c mice injected with miR-39 mimic (miR-39), transfection agent with miR-39 mimic (Trans-39) and miR-39 mimic loaded NPs (NP-39).

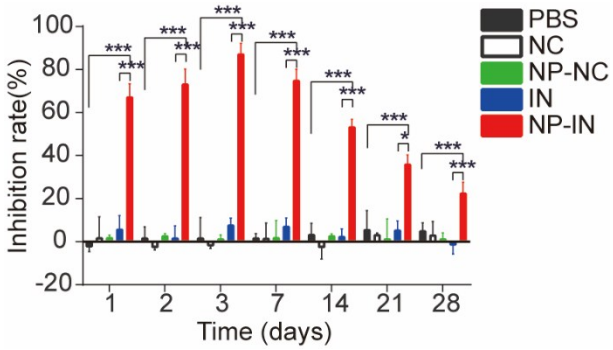

Fig. S15 Mice treated with different naked IN, transfection agent and NP-IN, miR-122 inhibition were measured.

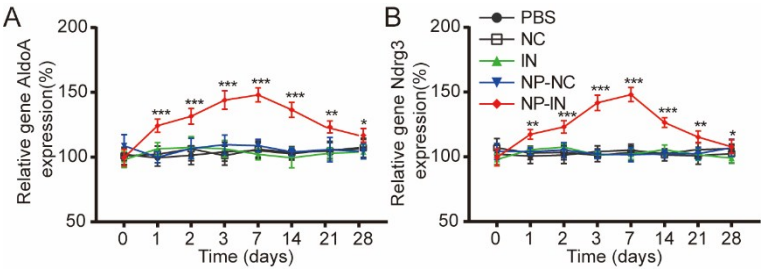

Fig. S16 *In vivo* miR-122 knockdown efficiency and relative gene expression after injected with NP-IN. (A) The Aldoa gene expression after injected with NP-IN. (B) The Aldoa gene expression after injected with NP-IN.

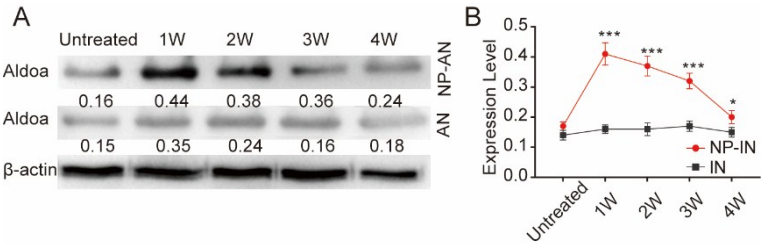

Fig. S17 (A) The Aldoa protein expression after different treatments. Aldoa protein level increased dramatically within 3 weeks after administrated with NP-IN. (B) Quantitative results of A. Naked IN group, there was no significant change compared to the control; The NP-IN also have strong influence on Aldoa protein.

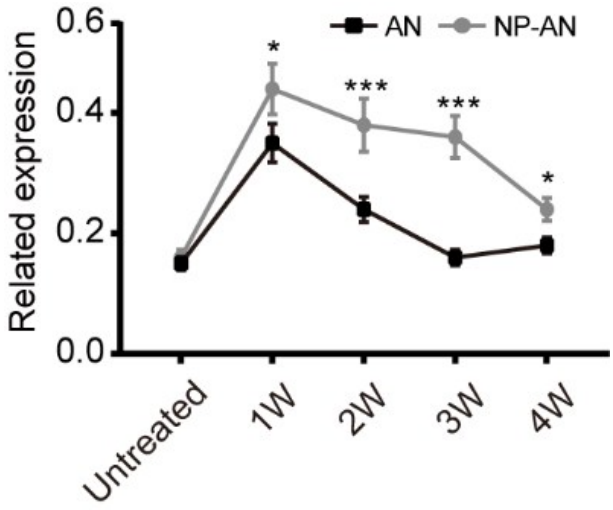

Fig. S18 Quantitative results of NP-AN, which showed that it have strong influence on Aldoa protein than free AN.

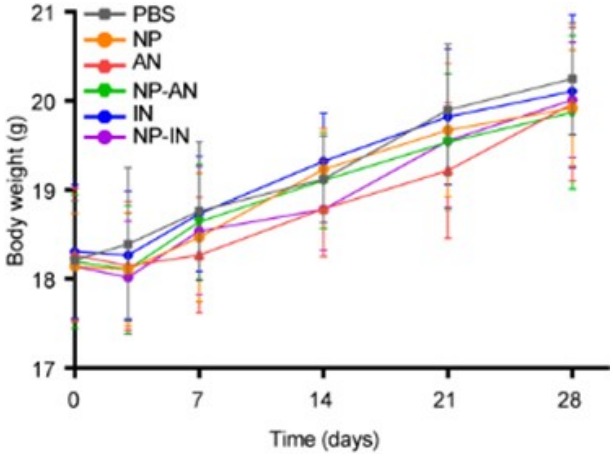

Fig. S19 Body weight changes after administrated with PBS, blank NP, AN, IN NP-AN and NP-IN. All groups showed no significant impact on the body weight of mice. PBS, AN, NP-AN, IN and NP-IN means injected with PBS, antagomir-122, antagomir-122 loading nanoparticles, inhibitor-122 and inhibitor-122 loading nanoparticles.

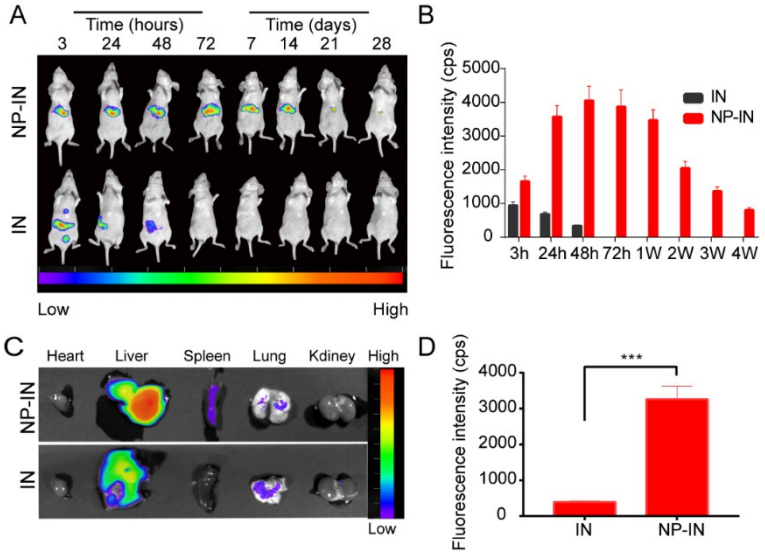

Fig. S20 *In vivo* targeting and organ distribution of NP-IN. (A) Fluorescence images of mice after i.v. administered NP. NP-IN could retained at liver for over 28 days, as the fluorescence results showed, while the IN retained only for 1 days. (B) Quantitative results of mice after different treatments. Further confirmed the results of A. Data are presented as the means ± SD. (n=6). (C) Ex vivo fluorescence images of organs harvested from treated mice at 72 h. NP-IN targeted at liver. Fluorescence of IN was much lower than NP-IN and even detected at lung. (D) Quantitative results of organs harvested from mice after 72 h of treatments. Further confirmed the results showed at B. Data are presented as the means ± SD. (n=6). *P<0.05, **P<0.01, ***P<0.005. IN and NP-IN means injected with inhibitor-122 and inhibitor-122 loading nanoparticles.

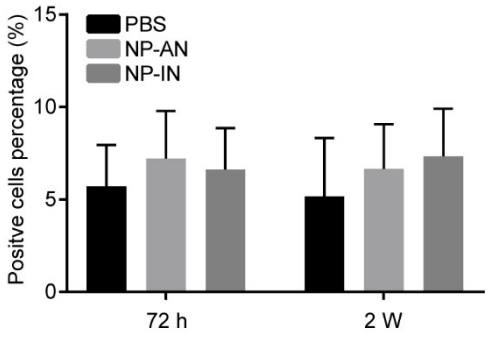

Fig. S21 Quantification of TUNEL assay. No obvious apoptosis was observed in NP-AN and NP-IN comparing to PBS group. *P<0.05, **P<0.01, ***P<0.005.

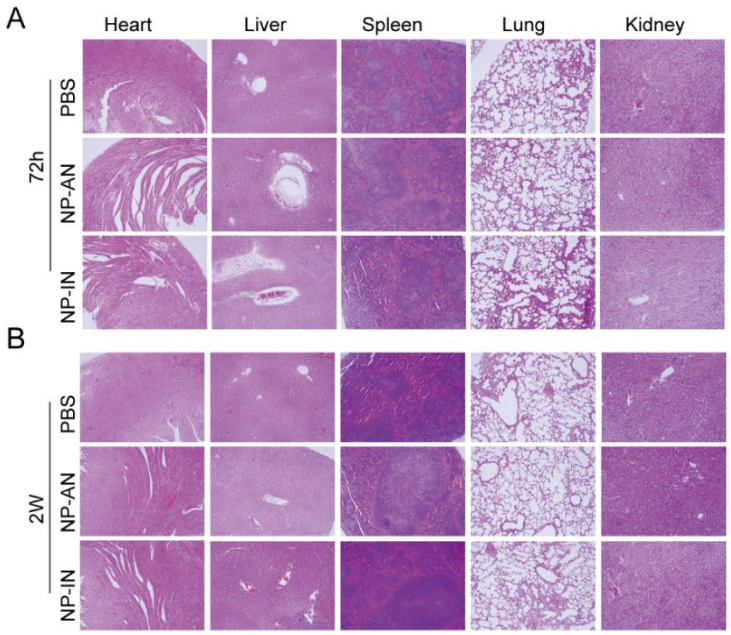

Fig. S22 HE staining of organs obtained from treated mice at 72 hours (A) and 2 weeks (B). No apparent tissue damage could be observed in both 72 hours and 2 week HE slices.